ELSEVIER

Polymer 42 (2001) 8817–8824

polymer

www.elsevier.com/locate/polymer

New ion conducting systems based on star branched block copolymer

A. Mokrini, J.L. Acosta*

Instituto de Ciencia y Tecnología de Polímeros, C/Juan de la Cierva 3, 28006 Madrid, Spain

Received 7 December 2000; received in revised form 5 April 2001; accepted 6 April 2001

Abstract

A new proton-conducting polymer based on sulfonated hydrogenated poly(styrene–butadiene) star block copolymer (HPBSE–SH) has been synthesized and characterized. The free acid samples and their blends with the non-sulfonated polymer (HPBSE) and Polypropylene (PP) were studied. The effect of sulfonation on polymer structure was studied using FTIR. Dynamic mechanical analysis and differential scanning calorimetry have been used for microstructure characterization. Glass transition temperatures of polystyrene (PS) measured through DMA present an increase about 45°C after sulfonation and an augmentation (10–20°C) as the PP content in HPBSE–SH/PP blends increases. Non-isothermal crystallization of PP was studied using Avrami analysis. Complex impedance measurements have shown that proton conductivity of HPBSE–SH was about 10^{-2} S cm^{-1} after hydration, lower values were observed generally in the case of blends. © 2001 Published by Elsevier Science Ltd.

Keywords: Proton conductor; Star branched poly(butadiene–styrene); Sulfonation

1. Introduction

Extensive studies have been performed to develop new ion conducting polymer electrolytes from aromatic polymer systems [1–5]. Selective aromatic ring sulfonation is a method offering good potential possibilities in this way.

Star branched poly(butadiene–styrene) block copolymer (PBSE) possesses a two-phase microstructure consisting of polystyrene domains dispersed in a rubbery continuous phase. One way to increase the performance of conventional block copolymer thermoplastic elastomers is to crosslink the PS microdomains, but to avoid the cross-linking/cyclization reaction of the high reactive carbon double bonds of the polybutadiene moiety, full hydrogenated systems should be used in order to avoid secondary reactions.

Several investigations have been devoted to study the morphology, chemical and physical properties of sulfonated polymer salts [6–9]. In this paper, we focus on the behavior of free acid form polymer and its blend with the non-sulfonated starting polymer and polypropylene. Polymer blends have become important to many industries, particularly when the concept of physical blending of two or more polymers allows obtaining of new products or problems solving [10]. Polypropylene was selected in this work to increase dimensional stability of the modified polymer and to improve processing conditions. The sulfonated polymers systems present a new physical network formed by ion-rich domain.

2. Experimental

2.1. Materials

The polymer used in this work was a selectively hydrogenated poly(butadiene–styrene) star branched block copolymer (HPBSE). The polymer commercially named Calprene, was provided by Repsol, has an average molecular weight ($\bar{M}_w$) 150 000 and contains 30 wt% styrene units. Sulfonating reagent was acetyl sulfate prepared by the reaction of acetic anhydride and concentrated sulfuric acid (96%). Sulfonation was carried out in 1,2-dichloroethane, previously dried using molecular sieve to remove any water that might have been present.

2.2. Sulfonation procedure

Acetyl sulfate preparation: acetic anhydride was cooled below −10°C, and the corresponding volume of 96% sulfuric acid was added. The solution was stirred, and finally 1,2-dichloroethane (DCE) was added. The reactive obtained was maintained at 0°C in an ice bath, until it was added to the reaction medium.

Sulfonation reaction: sulfonation was carried out according

* Corresponding author. Tel.: +34-91-562-29-00; fax: +34-91-564-48-53.

E-mail address: acosta@ictp.csic.es (J.L. Acosta).

0032-3861/01/$ - see front matter © 2001 Published by Elsevier Science Ltd.
PII: S0032-3861(01)00267-1

to the procedure described by Makowski et al. [12,13]. In an agitated reactor, the polymer was dissolved in DCE at 52–56°C and purged with nitrogen. Then, acetyl sulfate prepared as described above was added. The solution was stirred and purged with nitrogen during the experiment. Reaction was ended after 3 h reaction time and reaction product was recovered by precipitation in desionized water (1 l per 10 g of polymer used). The sulfonated polymer was filtered, washed many times with desionized water to ensure the complete removal of residual acid from the final product, and finally vacuum dried at 50–60°C for few days.

2.3. Membranes performing

For blends preparation, two procedures were used in this study. For HPBSE–SH/HPBSE blends, an open two-roll mill (friction 1:1.4) was utilized, using a conventional mixing procedure. The blending time was 20 min, to secure a good intermixture of the polymers.

In the case of HPBSE–SH/PP, since polypropylene is a crystalline polymer, a Brabender torque rheometer was used for blends preparation. First PP was melt in the thermoplastic mixing chamber preheated at 180°C, then HPBSE–SH was added using 60 rpm rotor speed. The material remained in the mixing chamber for 10 min, to ensure homogenization.

Membranes were performed by molding the materials between Teflon sheets in a Collin 600 hydraulic press at a temperature of 140–150°C and 200 bars pressure. Films obtained were 200–400 μm thickness.

2.4. Characterization

A Nicolet 520 Fourier-Transform-IR (FTIR) Spectrometer was used to record the infrared spectra of HPBSE polymer before and after sulfonation. A resolution setting of 4 cm^{-1} and 32 scans were utilized. Samples were swelled in chloroform and cast as thin films.

Photoelectron spectra were acquired with a VG ESCALAB 200R spectrometer provided with MgKα radiation ($h\nu = 1253.6$ eV) and a hemispherical electron analyzer. The spectrometer was calibrated using the Cu $^2p_{3/2}$ and the Au $^4f_{7/2}$ peaks of a metallic sample. The C ls, S 2p and O ls core-level spectra were recorded in kinetic energy (KE) ranges at pass energy of 20 eV. Each spectral region was scanned between 40 and 100 times, depending on the intensity of the signal, in order to get an acceptable signal-to-noise ratio at reasonable acquisition times.

A Mettler differential scanning calorimeter 30 (DSC) apparatus calibrated with indium was used for thermal analysis of the samples. To determine the glass transition (T_g), samples were first heated to 250°C at 30°C/min, then cooled to −140°C at 100°C/min, held at this temperature for 5 min, and then scanned at 10°C/min from −140 to 250°C. For the non-isothermal crystallization, samples were heated to 250°C at 30°C/min, held at this temperature for 2 min, and then scanned at slow rates from 250 to 40°C. The scanning rates used were 2, 4, 6, 8 and 10°C/min. All the measurements were carried out under nitrogen atmosphere.

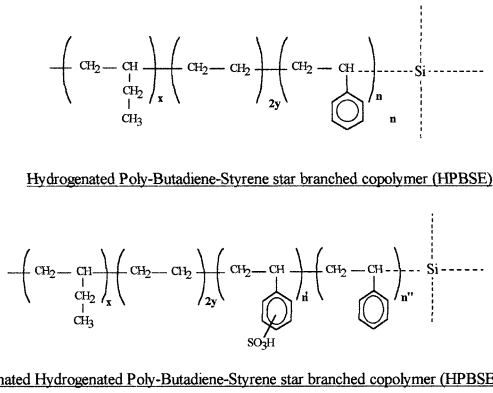

Fig. 1. Chemical mechanisms of sulfonation reaction of hydrogenated poly(butadiene–styrene) star branched copolymer.

Dynamic mechanical analysis (DMA) measurements were performed with a TA Instrument 2980 Dynamic Mechanical Analyzer, operating in the fixed frequency and film tension mode. The frequency used was 1 Hz and the temperature was varied from −100 to 300°C using a heating rate of 5°C/min.

A Hewlett Packard 4192A Impedance Spectroscopy Analyzer was used for impedance spectroscopy analysis of the samples. Complex impedance measurements were carried out in AC mode, in the frequency range 0.01–10 000 kHz, and 1 V amplitude of the applied AC signal. Samples were painted with Ag thin film (ceramic luster 200 in xylene supplied by EMETRON), to optimize the electrode–electrolyte interface, and sandwiched between two brass blocking electrodes in the measurement cell.

For impedance analysis, hydration procedure used consists in immersing samples in desionized water at 50°C

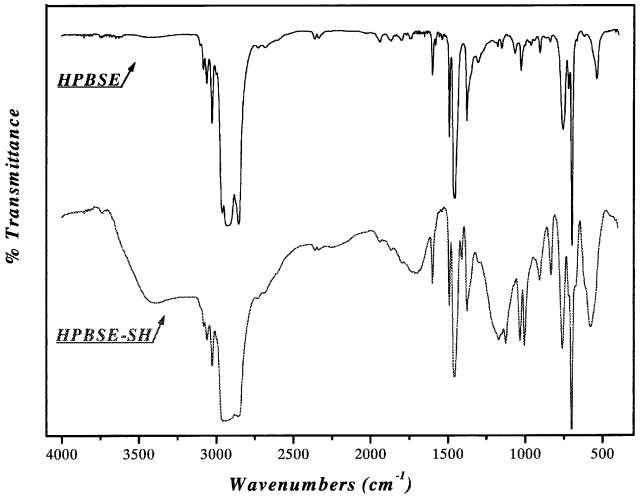

Fig. 2. FTIR spectra of HPBS before and after sulfonation. Resolution settings 4 cm^{-1}. 32 scans.

Table 1
Binding energies (eV) of core electrons, surface atomic ratios and sulfonation conversion of the samples

Samples	C 1s (eV)	O 1s (eV)	S 2p (eV)	S/C atom	Abundance SO_3H groups (%)
HPBSE	284.9 (83)	532.6 (85)	168.8	0.0033	1.70
	285.9 (17)	533.9 (15)			
AME-10	284.9 (79)	532.9 (68)	168.9	0.0301	15.75
	285.8 (21)	534.2 (32)			

for the required time. Before starting measurements, they were dried up superficially properly, and then placed in the measurement cell.

3. Results and discussion

3.1. HPBSE sulfonation

Sulfonation of star branched copolymer HPBSE was carried out according to the procedure described above. Fig. 1 shows the chemical mechanisms of the reaction.

FTIR was used to confirm the partial sulfonation of the styrene groups of the polymer. Fig. 2 compares a series of FTIR spectra before (HPBSE) and after sulfonation (HPBSE–SH). As can be seen, changes in the combination vibrations (finger bands) between 1950 and 1650 cm^{-1}, particularly characteristics of the phenyl group, are observed. The band centered around 1200 cm^{-1} is characteristic of the O=S=O asymmetric stretching vibration. Absorbencies at 1005 and 1126 cm^{-1} result, respectively from the vibrations of phenyl ring substituted with a sulfonic group and sulfonic anion attached to phenyl ring [7].

Photoelectron spectroscopy (XPS) has been used to determine the chemical state of the elements at the polymer surface and to quantify their abundance. Sulfonated hydrogenated polybutadiene styrene linear block copolymer samples, labeled AME-10, together with non-sulfonated sample labeled HPBSE as reference, have been used. Fig. 3 displays C 1s, O 1s, and S 2p core level spectra of the samples. The corresponding binding energies are summarized in Table 1. In order to measure the abundance of sulfonic groups (percentage of sulfonated styrene groups in relation to the 100% of all present monomer units), atomic S/C ratios have been calculated for all the samples and are summarized in Table 1. The results show that percentage of sulfonated styrene groups is 15.75% for sulfonated polymer and 1.70% for starting polymer, which is attributed to sulfur impurity of the sample.

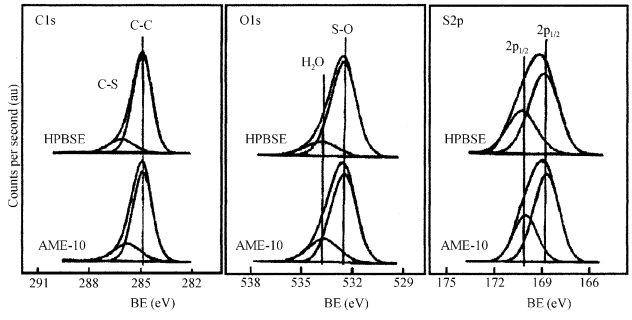

Fig. 3. C 1s, O 1s, and S 2p core level spectra of HPBSE and AME-10 samples.

For this study, sulfonated polymer (HPBSE–SH) was kept in its acid form, blends of HPBSE–SH with the non-sulfonated polymer (HPBSE) and polypropylene (PP) have been prepared. Table 2 lists the composition of all the materials used.

3.2. DMA and DSC analysis; glass transition temperatures

The primary focus of this mechanical analysis was to evaluate the effect of different factors on the structure of the samples. Fig. 4a and b shows the loss tangent (tan δ) versus temperature profiles for sulfonated polymer, containing different concentrations of pure polymer and polypropylene, respectively.

It can be seen that all the materials analyzed show the presence of two principal transitions, the lower one is associated with glass transition temperature of the hydrogenated polybutadiene HPB blocks, and the higher one with that of polystyrene PS domains. A larger tan δ peak is observed for the sulfonated samples. In addition, a new transition related to ion aggregations (multiplets or clusters) is observed in some of the samples containing sulfonated polymer (AME-13 and AME-23) at high temperature region (270°C).

Differential scanning calorimetry technique has shown a lower sensitivity compared with DMA as can be seen in Fig. 5, only low glass transition temperatures associated to HPB unit and melting temperature of PP could be determined.

Glass transition temperatures, defined as the inflection

Table 2
Composition of the samples

Sample name	HPBSE–SH (wt%)	HPBSE (wt%)	PP (wt%)
AME-10	100	–	–
AME-11	90	10	–
AME-12	80	20	–
AME-13	70	30	–
AME-21	90	–	10
AME-22	80	–	20
AME-23	70	–	30
AME-23*	–	70	30

* Sample used for DMA analysis.

point in DSC thermograms and as the maximum signal of tan δ in DMA, are summarized in Table 3.

It can be observed that glass transition temperature associated to hydrogenated polybutadiene units $T_{g\ (HPB)}$, is insensitive to sulfonation and blending; the maximum variation observed is about 4°C, while $T_{g\ (PS)}$ related to styrene blocks increased considerably (+45°C) after sulfonation ($T_{g\ (PS)} = 88$°C for HPBS and 133°C for HPBSE–SH). The augmentation in glass transition temperature is directly associated to ion content [11]. This is probably a result of the restrictions on the segmental movements in the styrene blocks, due to the hydrogen bounding of sulfonic groups introduced. $T_{g\ (PS)}$ in HPBSE–SH/HPBSE blends are included in the range between glass transition temperatures of both polymers, and decreases while the amount of HPBSE added to the sulfonated polymer increases.

The transition related to the cluster phase occurs between

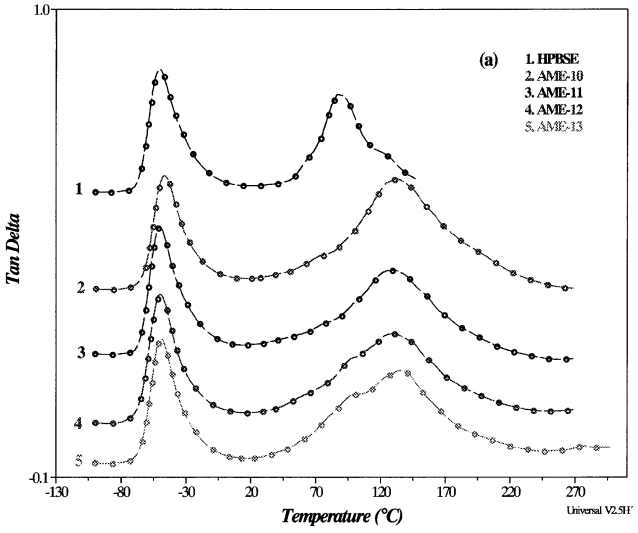

Fig. 4. DMA spectra obtained at 1 Hz frequency. Temperature range −100 to 290°C. Heating rate 5°C/min. (a) HPBSE–SH/HPBSE blends. (b) HPBSE–SH/PP blends.

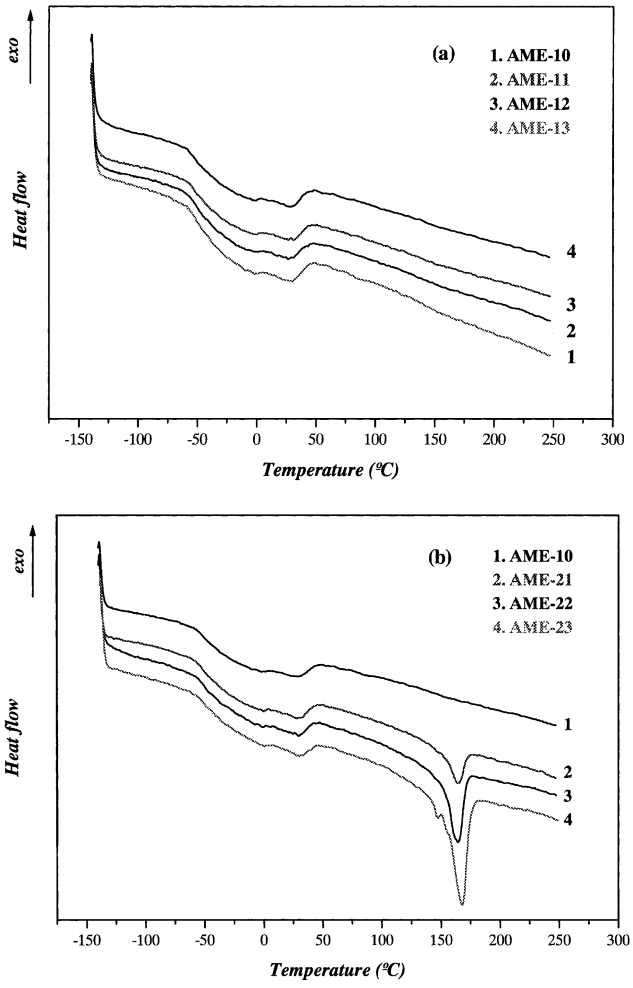

Fig. 5. DSC thermograms. Scanning rate 10°C/min. Temperature range −140 to 250°C. (a) HPBSE–SH/HPBSE blends. (b) HPBSE–SH/PP blends.

250 and 300°C, and it was not observed in all the samples. The disappearance of the transition related to clusters in the high temperature region indicates that damage was done to this phase of blend, or changes in structure due to the processing conditions.

For HPBSE–SH/PP blends, the same tendency is observed for $T_{g\ (HPB)}$, while in the case of $T_{g\ (PS)}$, in addition

Table 3
Glass transition temperatures through DMA and DSC

Sample name	DMA		DSC	
	$T_{g\ (PS)}$ (K)	$T_{g\ (PHB)}$ (K)	$T_{g\ (PHB)}$ (K)	$T_{m\ (PP)}$ (K)
HPBSE	87.65	−50.65	−50.80	–
AME-10	133.25	−46.35	−50.60	–
AME-11	128.45	−50.25	−50.50	–
AME-12	129.75	−49.55	−50.50	–
AME-13	129.95	−49.15	−52.60	–
AME-21	145.35	−47.05	−50.50	164.20
AME-22	140.85	−48.35	−50.40	164.20
AME-23	159.95	−50.95	−50.60	165.40

to the variation due to sulfonation, augmentation up to 28°C is noticed due to the incorporation of polypropylene to the sulfonated polymer. An increase in $T_{g\,(PS)}$ is viewed as the PP content increases, consequence of the introduction of crystalline component that limits chains movements and lead to differences in the degree of hydrogen bounding in the samples. However no changes in PP melting temperature are observed, which means that polymers are not miscible. From a technological point of view, molded membranes made from the blends show compatibility when PP content $\leq$30%, since membranes have good mechanical integrity and lower thickness as can be observed in Table 5.

3.3. Non-isothermal crystallization kinetics

Study of crystallization and melting behavior of crystallizable blends is a useful way to obtain information about miscibility, compatibility and microstructure behavior of polymer blends. In general, studies of crystallization are limited to idealized conditions, in which external conditions are constants (isothermal crystallization), for an easier theoretical analysis. However, practical processes, such as extrusion, molding and film forming usually occur under dynamic non-isothermal conditions, consequently, it will be useful to have a quantitative evaluation of the non-isothermal crystallization parameters.

Polypropylene is a polymorphic material with several crystal modifications [17], the appearance of these structures is critically dependent on crystallization conditions. Thermograms obtained for the blends studied show that crystallization of pure PP or from the melt HPBSE–SH/PP blends, depends greatly upon cooling rates and blends compositions. As shown in Fig. 6, for a given composition, crystallization process begins at higher temperatures when slower scanning rates are used. At a given cooling rate, the presence of HPBS–SH reduces the overall PP crystallization rate.

To describe the non-isothermal crystallization process of HPBS–SH/PP blends, the Avrami analysis was used [14–16].

$$\alpha(t) = 1 - \exp(-Kt^n) \tag{1}$$

where $\alpha(t)$ is the relative crystallinity as a function of temperature, K is a rate constant involving both nucleation and growth mechanisms, n is a parameter which also depends on the type of nucleation and the geometry of the growth process parameters, and t is crystallization time that can be determined in function of crystallization temperature T and cooling rate β.

$$t = \frac{T_0 - T}{\beta} \tag{2}$$

Plotting $\log[-\ln(1 - \alpha(t))]$ versus $\log(t)$ in Fig. 7, all the lines are parallel to each other, which means that the Avrami's equation is fulfilled. Intercept and slope values determined from the linear regression are, respectively, $\log K$ and the Avrami exponent n. All the data are listed in Table 4; the obtained correlation coefficients R are >99% for all the fits.

The values of $\log K$ obtained show that the crystallization rate increases with the increase in cooling rate for a given blend composition and decreases with the increase in PP content in the blends for a given cooling rate.

The value of Avrami exponent n contains information on nucleation and growth geometry, its interpretation may be complicated by factors due to the mechanisms involved during the process. As can be seen in Fig. 8, for a given

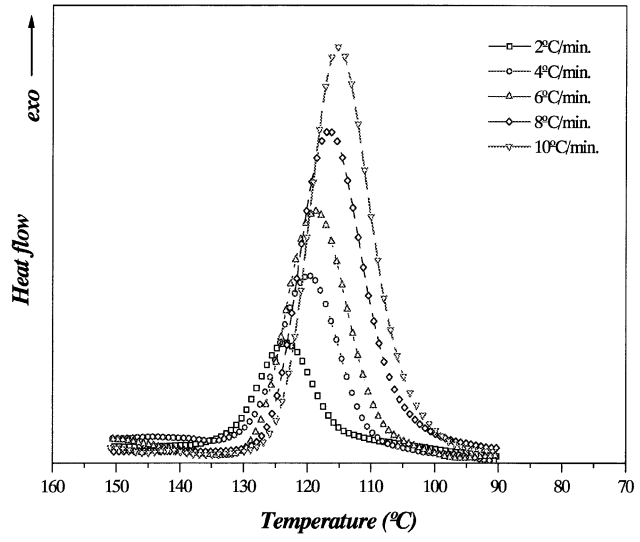

Fig. 6. Thermograms obtained by DSC at different scanning rates for the non-isothermal crystallization of PP in AME-21 blend. Temperature range 250–40°C.

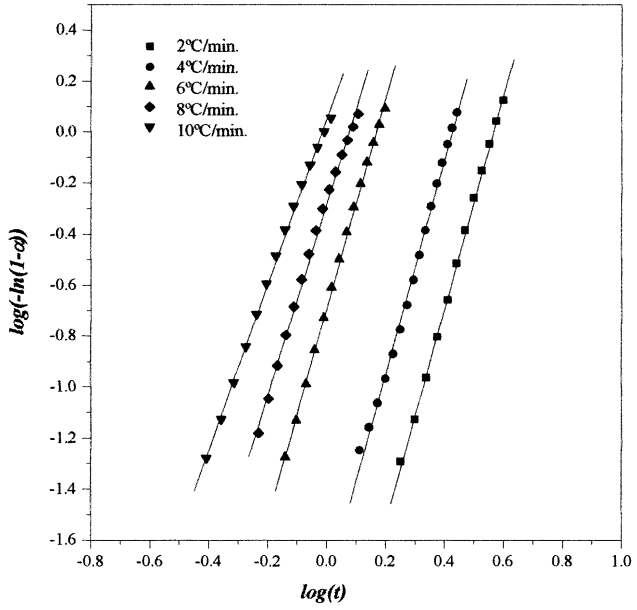

Fig. 7. Representation of Avrami's equation, for AME-21 blend (90% HPBSE–SH and 10% PP) at different scanning rates.

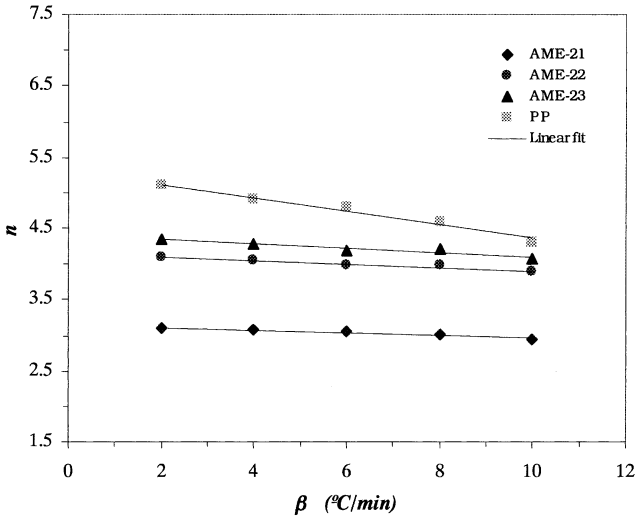

Fig. 8. Plot of Avrami exponent n versus cooling rate β for non-isothermal crystallization of PP pure and in HPBSE–SH/PP blends with different PP content.

Table 4
Kinetic parameters obtained from the application of Avrami's equation for non-isothermal crystallization of PP in HPBSE–SH/PP blends

Sample	β (°C/min)	log K	n	R
AME-21	2	−2.74	3.10	99.46
	4	−1.26	3.08	99.98
	6	−0.84	3.05	99.94
	8	−0.52	3.02	99.99
	10	−0.32	2.95	99.99
AME-22	2	−3.37	4.09	99.77
	4	−1.89	4.06	99.87
	6	−1.38	3.97	99.94
	8	−0.85	3.97	99.96
	10	−0.5	3.89	99.95
AME-23	2	−3.37	4.35	99.92
	4	−1.98	4.27	99.89
	6	−1.52	4.18	99.87
	8	−0.63	4.20	99.94
	10	−0.34	4.08	99.88
PP	2	−3.24	5.1	99.95
	4	−1.83	4.9	99.80
	6	−1.22	4.8	99.93
	8	−0.91	4.6	99.81
	10	−0.51	4.3	99.59

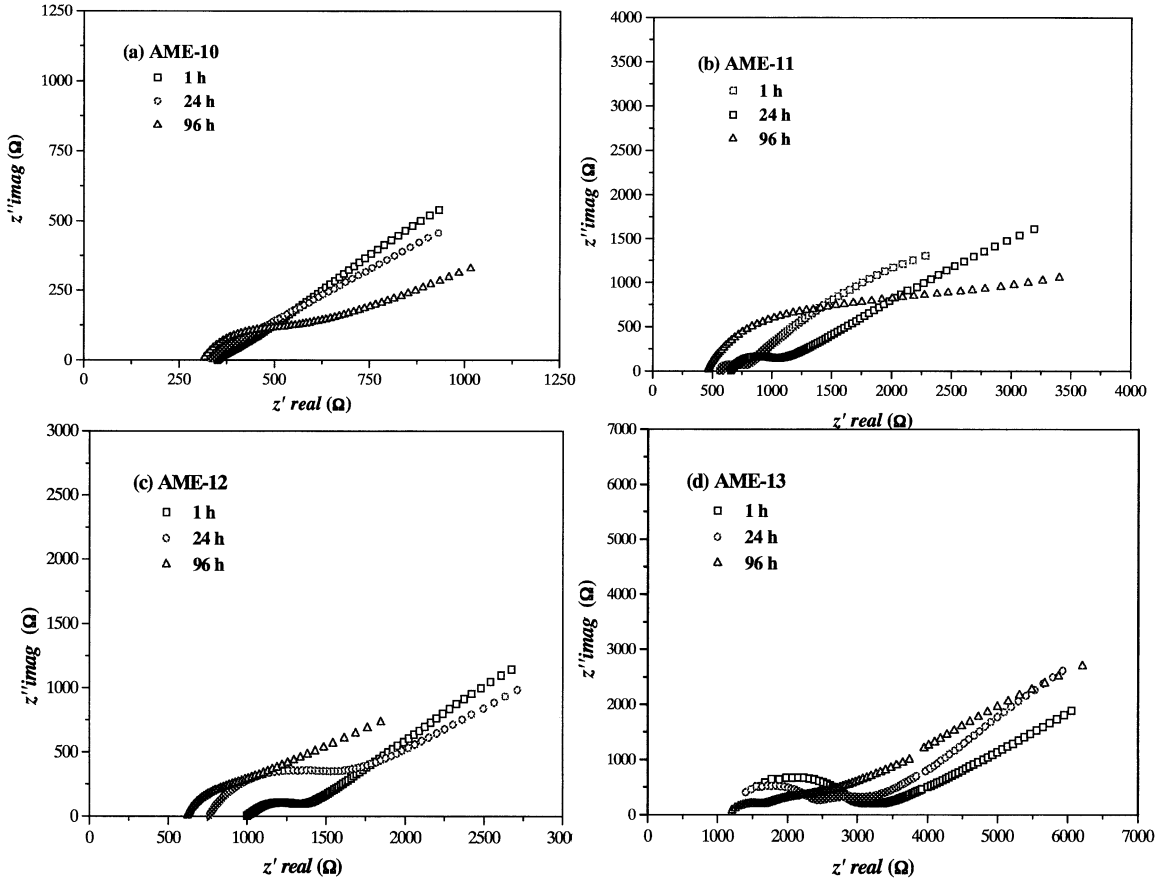

Fig. 9. Impedance spectra obtained for HPBSE–SH/HPBSE blends after 1, 24 and 96 h hydration time at 50°C. AC mode. 1 V amplitude of applied signal. Frequency range 0.01–10 000 kHz. (a) AME-10 membrane. (b) AME-11. (c) AME-12. (d) AME-13.

Table 5
Conductivity data before and after hydration at 50°C

Sample name	Thickness mem. (μm)	Conductivity before hydration (S cm^{-1})	Conductivity after hydration (S cm^{-1})		
			1 h	24 h	69 h
AME-10	370	5.5×10^{-8}	1.1×10^{-2}	4.1×10^{-3}	3.8×10^{-3}
AME-11	320	6.6×10^{-8}	4.9×10^{-3}	2.0×10^{-3}	1.1×10^{-3}
AME-12	310	3.7×10^{-8}	3.1×10^{-3}	9.3×10^{-4}	2.2×10^{-3}
AME-13	290	9.2×10^{-8}	5.1×10^{-4}	7.3×10^{-4}	1.5×10^{-3}
AME-21	340	4.2×10^{-9}	6.4×10^{-4}	2.1×10^{-3}	4.2×10^{-4}
AME-22	320	4.4×10^{-9}	2.1×10^{-4}	6.0×10^{-3}	1.8×10^{-3}
AME-23	310	3.9×10^{-9}	2.1×10^{-4}	7.1×10^{-4}	9.2×10^{-4}
Comercial Nafion	180	5.3×10^{-4}	2.0×10^{-3}	2.0×10^{-2}	1.3×10^{-1}

composition, n remains practically constant and does not depend on cooling rates, except for pure PP where a decrease of n is observed increasing cooling rates. The general tendency observed is, higher values of n as PP content in the blends increases. This behavior can be explained by changes in growth geometry when the composition is varied.

Changes in n values observed are due to the transition between heterogeneous and homogeneous nucleation [17]. When PP content was about 10 wt%, the value of Avrami exponent was close to 3 and can be attributed to heterogeneous nucleation of a three-dimensional growth. For higher percentages (20–30%), n was close to 4, which suggested that the non-isothermal crystallization of PP in HPBSE–SH/PP blends correspond to a three-dimensional growth with homogeneous nucleation.

3.4. Conductivity analysis

Ionic conductivity of membrane was determined using the complex impedance method. Impedance spectrum, shown in Fig. 9, comprises two well-defined regions, a high frequency zone that is related to conduction processes in the bulk of the sample, and a low frequency region, which is attributed to the solid electrolyte–electrode interface. The bulk resistance is obtained from the intercept of high frequency curves with the real axis. This resistance is smaller for samples with higher conductivities.

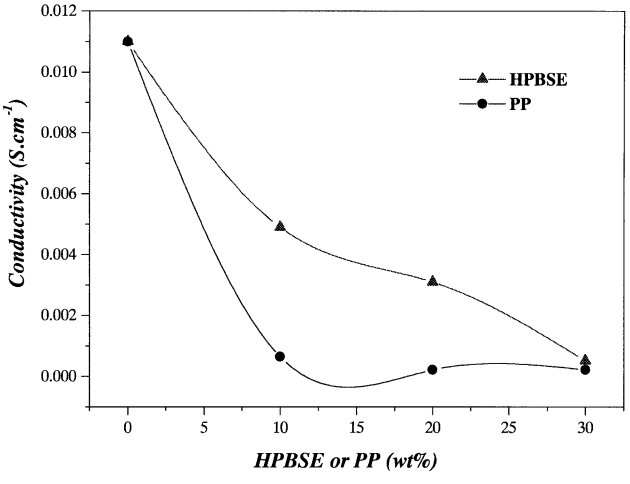

Fig. 10. Isotherms of ionic conductivity of HPBSE–SH blends as a function of HPBSE and PP content.

All impedance measurements were done before and after hydration of the films. Membranes in dry form exhibit conductivities between 10^{-8} and 10^{-9} S cm^{-1}, entire conduction process occurs through the water incorporated in polymer structure. Data obtained before and after hydration are represented in Table 5.

As shown, ionic conductivity of membranes increases several orders of magnitude after 1 h immersion in water, and remains within the same order of magnitude for higher hydration time. In Fig. 10, isotherms at 50°C of ionic conductivity of HPBSE–SH blends as a function of percentages of HPBSE and PP added are plotted. In all cases, a decrease in ionic conductivity is observed.

Results obtained have been compared with those of commercial Nafion, data obtained show in general higher conductivities for Nafion.

4. Conclusions

Sulfonated hydrogenated polybutadiene styrene star branched polymer HPBSE–SH, was prepared by partially sulfonating the styrene blocks. Spectroscopy FTIR confirms that styrene sulfate was the reaction product.

DMA analyses show that glass transition temperature of PS domain, increases 45°C after sulfonation, while T_g of hydrogenated polybutadiene phase remains practically constant.

For HPBSE–SH/HPBS blends, $T_{g\ (PS)}$ decreases when the amount of HPBS added increases. In the case of HPBS–SH/PP blends, compatibility between both polymers, and an augmentation in glass transition temperature (up to 27°C) as the PP content increases, were observed.

The study of non-isothermal crystallization kinetics of PP in HPBSE–SH/PP blends, using Avrami analysis, shows

that scanning rate has no influence on Avrami exponent values for a fixed composition. For the blend containing 10 wt% PP, n was close to 3 and could be attributed to heterogeneous nucleation. For higher PP concentrations used, Avrami exponent was approximately 4 and corresponds to a three-dimensional growth with homogeneous nucleation.

In the case of impedance analysis, all the samples before hydration present ionic conductivities in the range of 10^{-8}–10^{-10} S cm^{-1}. After hydration, conductivities increase several orders of magnitude, the higher value obtained was 10^{-2} S cm^{-1} and corresponds to AME-10 sample. The general tendency was a diminution of film thickness but also of electrical properties, increasing HPBS or PP content of the blends. Results obtained have been compared with those of commercial Nafion, data obtained show in general higher conductivities for Nafion.

Acknowledgements

The support of Repsol and the European Community is gratefully acknowledged.

References

[1] Scrosati B. Applications of electroactive polymers. London: Chapman & Hall, 1993.
[2] Jun YK, Seong HK. Solid State Ion 1999;124:91–99.
[3] Blythe AR. Electrical properties of polymers. New York: Cambridge University Press, 1979.
[4] Gray FM. Solid polymer electrolytes; fundamentals and technological applications. New York: VCH Publishers, 1991.
[5] Harsanyi G. Polymer films in sensor applications. Lancaster: Technomic, 1995.
[6] Weiss RA, Sen A, Pottick LA, Willis CL. Polymer 1991;32(15):2785–92.
[7] Weiss RA, Sen A, Willis CL, Pottick LA. Polymer 1991;32(10):1867–74.
[8] Nishida M, Eisenberg A. Macromolecules 1996;29:1507–15.
[9] Kim JS, Nishida M, Eisenberg A. Polym J 1999;31(1):96–8.
[10] Paul DR. Polymer blends. New York: Academic Press, 1978.
[11] Eisenberg A, Kim JS. Introduction to ionomers. New York: Wiley, 1998.
[12] Makowski HS, et al. US Patent 3 870 841; 1975.
[13] Makowski HS, et al. US Patent 4 184 988; 1980.
[14] Avrami M. J Chem Phys 1939;7:1103–9.
[15] Avrami M. J Chem Phys 1940;8:212–21.
[16] Avrami M. J Chem Phys 1941;9:177–85.
[17] Di Lorenzo ML, Silvestre C. Prog Polym Sci 1999;24:917–50.